Inorg. Chem. **2008**, *47*, 11057−11061

Structures and Magnetic Properties of Ferromagnetic Coupling 2D Ln−M Heterometallic Coordination Polymers (Ln = Ho, Er; M = Mn, Zn)

Hong-Ling Gao,[†] Bin Zhao,[†,‡] Xiao-Qing Zhao,[†] You Song,[‡] Peng Cheng,*[,†] Dai-Zheng Liao,[†] and Shi-Ping Yan[†]

Department of Chemistry, Nankai University, Tianjin 300071, P. R. China, and Coordination Chemistry Institute and the State Key Laboratory of Coordination Chemistry, Nanjing University, Nanjing 210093, China

Received July 18, 2008

Four new heterometallic coordination polymers have been successfully synthesized, namely, $\{[Ho_2(HCAM)_6Mn_3(H_2O)_{12}]\cdot 17.5H_2O\}_n$ (**1**), $\{[Er_2(HCAM)_6Mn_3(H_2O)_{12}]\cdot 17.5H_2O\}_n$ (**2**), $\{[Ho_2(HCAM)_6Zn_3(H_2O)_{12}]\cdot 26H_2O\}_n$ (**3**), and $\{[Er_2(HCAM)_6Zn_3(H_2O)_{12}]\cdot 26H_2O\}_n$ (**4**) (H_3CAM = chelidamic acid). X-ray crystallographic studies reveal that coordination polymers **1**−**4** are isostructural and crystallized in the rhombohedral crystal system, space group $R\bar{3}$. These compounds comprise a 2D honeycomb-type framework. A 2D water sheet is first found in **3** and **4**, which exhibits a novel topological motif. The magnetic results for **1**−**4** show that ferromagnetic interactions take place between the Ho^{3+}/Er^{3+} and Mn^{2+} ions within **1** and **2**.

Introduction

The rather large and anisotropic magnetic moments of some paramagnetic lanthanide ions have attracted much interest in the field of molecule-based magnetic materials.[1] Such magnetic anisotropy is required for magnetically ordered materials with large coercive fields such as hard magnets. For the past two decades or so, a large number of compounds containing both lanthanide and a second spin carrier such as transition metal ions or organic radicals have been described.[2] Although many of them were magnetically measured, the magnetic coupling nature (ferro- or antiferromagnetic) between Ln^{3+} ions (except for the isotropic Gd^{3+} ion) and another spin carrier was not determined explicitly. In 1985, Gatteschi et al. pioneered exploration of the nature of magnetic coupling between Gd^{3+} and Cu^{2+} ions,[2b] and then lots of examples of investigating the magnetic interaction between Gd^{3+} and Cu^{2+} ions were reported,[3,4] of which almost all show ferromagnetic coupling, with the exception of a few antiferromagnetic ones. Recently, Sutter et al. systematically studied the magnetic interactions between Ln^{3+} ions (Ln = Ce to Ho) and radicals.[2d,e] Up to now, however, analysis of the nature of magnetic coupling between Ln (Ln ≠ Gd) and other transition metal ions has been rather rare, since the application of a theoretical model to analyze

* Author to whom correspondence should be addressed. Fax: +86-22-23502458. E-mail: pcheng@nankai.edu.cn.
† Nankai University
‡ Nanjing University

(1) (a) Zhao, H.; Bazile, M. J.; Galán-Mascarós, J. R.; Dunbar, K. R. *Angew. Chem., Int. Ed.* **2003**, *42*, 1015. (b) Costes, J. P.; Clemente-Juan, J. M.; Dahan, F.; Nicodème, F.; Verelst, M. *Angew. Chem., Int. Ed.* **2002**, *41*, 333.

(2) (a) Winpenny, R. E. P. *Chem. Soc. Rev.* **1998**, *27*, 477. (b) Bencini, A.; Benelli, C.; Caneschi, A.; Carlin, R. L.; Dei, A.; Gatteschi, D. *J. Am. Chem. Soc.* **1985**, *107*, 8128. (c) Benelli, C.; Caneschi, A.; Gatteschi, D.; Sessoli, R. *J. Appl. Phys.* **1993**, *15*, 5333. (d) Kahn, M. L.; Sutter, J. P.; Golhen, S.; Guionneau, P.; Ouahab, L.; Kahn, O.; Chasseau, D. *J. Am. Chem. Soc.* **2000**, *122*, 3413. (e) Kahn, M. L.; Ballou, R.; Porcher, P.; Kahn, O.; Sutter, J. P. *Chem.—Eur. J.* **2002**, *8*, 525. (f) Kou, H. Z.; Zhou, B. C.; Gao, S. R.; Wang, J. *Angew. Chem., Int. Ed.* **2003**, *42*, 3288. (g) Prasad, T. K.; Rajasekharan, M. V.; Costes, J. P. *Angew. Chem., Int. Ed.* **2007**, *46*, 2851.

(3) For example:(a) Bencini, A.; Benelli, C.; Caneschi, A.; Dei, A.; Gateschi, D. *Inorg. Chem.* **1986**, *25*, 572. (b) Benelli, C.; Caneschi, A.; Gateschi, D.; Laugier, J.; Rey, P. *Angew. Chem., Int. Ed.* **1987**, *26*, 913. (c) Costes, J. P.; Dahan, F.; Dupuis, A. *Inorg. Chem.* **2000**, *39*, 5994. (d) Benelli, C.; Gatteschi, D. *Chem. Rev.* **2002**, *102*, 2369. (e) Margeat, O.; Lacroix, P. G.; Costes, J. P.; Donnadieu, B.; Lepetit, C. *Inorg. Chem.* **2004**, *43*, 4743. (f) Akine, S.; Matsumoto, T.; Taniguchi, T.; Nabeshima, T. *Inorg. Chem.* **2005**, *44*, 3270. (g) Koner, R.; Lin, H. H.; Wei, H. H.; Mohahtal, S. *Inorg. Chem.* **2005**, *44*, 3524. (h) Manna, S. C.; Konar, S.; Zangrando, E.; Ribas, J.; Chaudhuri, N. R. *Polyhedron* **2007**, *26*, 2507.

(4) (a) Baggio, R.; Garland, M. T.; Moreno, Y.; Pena, O.; Perec, M.; Spodine, E. *J. Chem. Soc., Dalton Trans.* **2000**, 2061. (b) Liu, Q. D.; Gao, S.; Li, J. R.; Ma, B. Q.; Zhou, Q. Z.; Yu, K. B. *Polyhedron* **2002**, *21*, 1097. (c) Zou, Y.; Liu, W. L.; Gao, S.; Lu, C. S.; Dang, D. B.; Meng, Q. J. *Polyhedron* **2004**, *23*, 2253. (d) Kou, H. Z.; Jiang, Y. B.; Cui, A. L. *Cryst. Growth Des.* **2005**, *5*, 77.

10.1021/ic801332a CCC: $40.75
Published on Web 10/29/2008

such magnetic interactions is impeded by the first-order orbital momentum of the Ln^{3+} ion, and the Heisenberg−Dirac−van Vleck phenomenological spin Hamiltonian is hence no longer appropriate to describe the low-lying states.[5] The difficulties in analyzing magnetic properties of the system associated with lanthanide ions have been discussed in detail.[2d]

On account of the repulsion among f electrons and spin−orbit coupling, the $4f^n$ configuration of Ln^{3+} ions may be split into $^{2S+1}L_J$ spectroscopic levels, which are further split into Stark sublevels by the crystal field perturbation.[6] The number of Stark energy levels was mainly determined by the site symmetry of the Ln^{3+} ions. At room temperature, it is possible for all Stark sublevels to be thermally populated. A depopulation of these sublevels will occur when the temperature is lowered, and consequently, $\chi_M^{Ln}T$ decreases (χ_M^{Ln} stands for the molar magnetic susceptibility of Ln^{3+} ions). When the Ln^{3+} ions interact with M (M = the second spin carrier), the temperature dependence of $\chi_M T$ results from both the variation of $\chi_M^{Ln}T$ and the coupling between Ln^{3+} and M. As a result, the nature of the magnetic interactions between Ln^{3+} and M cannot be unambiguously deduced, only in the case where $\chi_M T$ decreases with decreasing temperature. On the contrary, when the $\chi_M T$ value increases with the decreasing temperature, it is certain that magnetic interactions between Ln^{3+} and M shows ferromagnetic coupling.

In order to obtain new insight into the nature of the magnetic interactions between Ln^{3+} ions and the second spin carriers, Kahn et al. addressed the problem experimentally by the method of diamagnetic ion substitution.[7] Namely, when the magnetic properties of two isostructural complexes are compared (one contains Ln^{3+} and the second spin carrier, and the other contains Ln^{3+} and diamagnetic species), any change in the magnetic properties originated from differences of the molecular structures will be excluded, and the trouble caused by the spin−orbit coupling of the Ln^{3+} ions will also be eliminated. To date, the use of this method to study the magnetic interactions between Ln^{3+} ions and another paramagnetic species is very scarce.[7,8]

Recently, we have reported a series of Ln−Mn zeolite-type and molecular-ladder complexes based on pyridine-2,6-dicarboxylic acid (H_2dipic).[9] The ferromagnetic interaction between Tb^{3+} and Mn^{2+} ions was observed for the first time in the Ln−Mn system.[9c] Inspired by our previous work, a ligand, H_3CAM (chelidamic acid), with similarity to H_2dipic was employed in the hydrothermal synthesis, and two new 2D Ln−Mn complexes $\{[Ho_2(HCAM)_6Mn_3(H_2O)_{12}]\cdot 17.5H_2O\}_n$ (**1**) and $\{[Er_2(HCAM)_6Mn_3(H_2O)_{12}]\cdot 17.5H_2O\}_n$ (**2**) were obtained. In order to investigate the nature of magnetic coupling between Ln^{3+} (Ln = Ho, Er) and Mn^{2+}, diamagnetic Zn^{2+} was expected to substitute Mn^{2+} in **1** and **2** due to almost identical ionic radii of Mn^{2+} and Zn^{2+}. Fortunately, two corresponding Ln−Zn analogues, $\{[Ho_2(HCAM)_6Zn_3(H_2O)_{12}]\cdot 26H_2O\}_n$ (**3**) and $\{[Er_2(HCAM)_6Zn_3(H_2O)_{12}]\cdot 26H_2O\}_n$ (**4**), were successfully prepared. These polymers exhibit 2D honeycomb structures comprised of 48-membered rings (48MRs), possessing C_6 symmetry, and showing a unique 2D water sheet in **3** and **4**. Importantly, magnetic investigations for **1**−**4** reveal a rather rare ferromagnetic interaction between Ho^{3+} (or Er^{3+}) and Mn^{2+} ions, which has not been reported before.

Experimental Section

Physical Measurements. Analyses for C, H, and N were carried out on a Perkin-Elmer analyzer. Thermal gravimetric analyses were completed on a NETZSCH TG 209 instrument. Variable-temperature magnetic susceptibilities were measured on a Quantum Design MPMS-7 superconducting quantum interference device (SQUID) magnetometer. The sample holder is a capsule, and the data were corrected for the diamagnetic contributions of both the sample holder and the compound obtained from Pascal's constants.

Synthesis of 1−4. A mixture of Ho_2O_3 (0.2 mmol, 0.0378 g) or $Er(NO_3)_3\cdot 6H_2O$ (0.2 mmol, 0.0923 g), MSO_4 (0.3 mmol, M = Mn^{2+}, 0.0453 g; Zn^{2+}, 0.0484 g), H_2CAM (0.6 mmol, 0.1206 g), and H_2O (12 mL) was stirred for 1 h at room temperature and then was put in a 25 mL acid digestion bomb and heated at 180 °C (**1** and **2**) or 160 °C (**3** and **4**) for three days. The crystal products were collected after washing with H_2O (2 × 5 mL) and diethyl ether (2 × 5 mL). Elem anal. (%) calcd for $C_{42}H_{77}Ho_2N_6O_{59.5}Mn_3$ (**1**): C, 23.45; H, 3.76; N, 3.86%. Found: C, 23.88; H, 3.67; N, 3.98%. Elem anal. (%) calcd for $C_{42}H_{77}Er_2N_6O_{59.5}Mn_3$ (**2**): C, 23.55; H, 3.75; N, 3.89%. Found: C, 23.82; H, 3.66; N, 3.97%. Elem anal. (%) calcd for $C_{42}H_{88}Ho_2N_6O_{68}Zn_3$ (**3**): C, 23.45; H, 3.76; N, 3.86%. Found: C, 22.01; H, 3.87; N, 3.67%. Elem anal. (%) calcd for $C_{42}H_{88}Er_2N_6O_{68}Zn_3$ (**4**): C, 21.59; H, 3.73; N, 3.81%. Found: C, 21.97; H, 3.86; N, 3.66%.

Crystallographic Studies. Single-crystal X-ray diffraction measurements of complexes **1**−**4** were carried out with a Bruker Smart CCD diffractometer and an APEX II CCD area detector equipped with a graphite crystal monochromator situated in the incident beam for data collection at 293(2) K. The structures were solved by direct methods and refined by full-matrix least-squares techniques using

(5) Kahn, O. *Molecular Magnetism*; VCH: New York 1993.
(6) Bünzli, J. C. G.; Chopin, G. R. *Lanthanide probes in life, chemicals and earth sciences: theory and practice*; Elsevier: Amsterdam, The Netherlands, 1989.
(7) (a) Kahn, M. L.; Mathoniére, C.; Kahn, O. *Inorg. Chem.* **1999**, *38*, 3692. (b) Sutter, J. P.; Kahn, M. L.; Kahn, O. *Adv. Mater.* **1999**, *11*, 863. (c) Kahn, M. L.; Lecante, P.; Verelst, M.; Mathoniere, C.; Kahn, O. *Chem. Mater.* **2000**, *12*, 3073.
(8) (a) Ma, B. Q.; Gao, S.; Su, G.; Xu, G. X. *Angew. Chem., Int. Ed.* **2001**, *40*, 448. (b) Figuerola, A.; Diaz, C.; Ribas, J.; Tangoulis, V.; Granell, J.; Lloret, F.; Mahia, J.; Maestro, M. *Inorg. Chem.* **2003**, *42*, 641. (c) Costes, J. P.; Dahan, F.; Dupuis, A.; Laurent, J. R. *Chem.—Eur. J.* **1998**, *4*, 1616. (d) Caneschi, A.; Sorace, L.; Casellato, U.; Tomasin, P.; Vigato, P. A. *Eur. J. Inorg. Chem.* **2005**, 3887. (e) Chen, W. T.; Guo, G. C.; Wang, M. S.; Xu, G.; Cai, L. Z.; Akits, T.; Akit-Tanaka, M.; Matsushita, A.; Huang, J. S. *Inorg. Chem.* **2007**, *46*, 2105.
(9) (a) Zhao, B.; Cheng, P.; Dai, Y.; Cheng, C.; Liao, D. Z.; Yan, S. P.; Jiang, Z. H.; Wang, G. L. *Angew. Chem., Int. Ed.* **2003**, *42*, 934. (b) Zhao, B.; Cheng, P.; Chen, X. Y.; Cheng, C.; Shi, W.; Liao, D. Z.; Yan, S. P.; Jiang, Z. H. *J. Am. Chem. Soc.* **2004**, *126*, 3012. (c) Zhao, B.; Chen, X. Y.; Cheng, P.; Liao, D. Z.; Yan, S. P.; Jiang, Z. H. *J. Am. Chem. Soc.* **2004**, *126*, 15394. (d) Zhao, B.; Gao, H. L.; Chen, X. Y.; Cheng, P.; Shi, W.; Liao, D. Z.; Yan, S. P.; Jiang, Z. H. *Chem.—Eur. J.* **2006**, *12*, 149.

Table 1. Crystal Data and Structure Parameters for **1**−**4**

	1	**2**	**3**	**4**
empirical formula	$C_{42}H_{77}Ho_2N_6O_{59.5}Mn_3$	$C_{42}H_{77}Er_2N_6O_{59.5}Mn_3$	$C_{42}H_{88}Ho_2N_6O_{68}Zn_3$	$C_{42}H_{88}Er_2N_6O_{68}Zn_3$
fw	2112.78	2117.44	2291.15	2295.81
temp (K)	293(2)	293(2)	293(2)	293(2)
λ/Å	0.71073	0.71073	0.71073	0.71073
cryst syst	rhombohedral	rhombohedral	rhombohedral	rhombohedral
space group	$R\bar{3}$	$R\bar{3}$	$R\bar{3}$	$R\bar{3}$
a (Å)	14.419(2)	14.453(3)	14.305(7)	14.27(2)
b (Å)	14.419(2)	14.453(3)	14.305(7)	14.27(2)
c (Å)	34.057(10)	34.208(12)	35.075(15)	34.75(6)
γ (deg)	120.00	120.00	120°	120°
vol/Å^3	6132 (2)	6188(3)	6216(5)	6128(16)
Z	3	3	3	3
density (calcd) (Mg/m^3)	1.716	1.705	1.836	1.866
abs coeff (mm^{-1})	2.478	2.571	2.869	3.028
$2\theta_{max}$ (°)	52.86	52.86	50.02	50.02
limiting indices	$-4 \le h \le 18$	$-9 \le h \le 18$	$-17 \le h \le 12$	$-16 \le h \le 15$
	$-18 \le k \le 14$	$-18 \le k \le 17$	$-16 \le k \le 17$	$-16 \le k \le 16$
	$-40 \le l \le 31$	$-42 \le l \le 42$	$-34 \le l \le 41$	$-40 \le l \le 25$
reflns collected/unique	6528/2750	11892/ 2835	10556/2438	10446/2397
	[R(int) = 0.0360]	[R(int) = 0.0830]	[R(int) = 0.1125]	[R(int) = 0.0916]
data/restraints/params	2750/36/188	2835/36/189	2438/0/ 193	2397/ 0/193
GOF on F^2	1.082	1.102	1.102	1.121
R1, wR2 [I > 2σ (I)]	0.0369, 0.1034	0.0472, 0.1211	0.0396, 0.0935	0.0370, 0.0718
R1, wR2 (all data)	0.0476, 0.1098	0.0763, 0.1421	0.0519, 0.1028	0.0535, 0.0762
largest diff. peak and hole [e Å^{-3}]	1.276/−0.514	0.975/−0.583	0.608/−0.829	0.783/−0.803

the SHELXS-97 and SHELXL-97 programs.[10] Anisotropic thermal parameters were assigned to all non-hydrogen atoms. The hydrogen atoms were placed in idealized positions and located in the difference Fourier map. The crystallographic data for **1**−**4** are listed in Table 1.

CCDC-227158 (**1**), -225277 (**2**), -250745 (**3**), and -238885 (**4**) contain the supplementary crystallographic data for this paper. These data can be obtained free of charge at www.ccdc.cam.ac.uk/data_request/cif (or from the Cambridge Crystallographic Data Centre, 12 Union Rd., Cambridge CB2 1EZ, U.K., fax (+44) 1223−336033, e-mail deposit@ccdc.cam.ac.uk).

Results and Discussion

Crystallography. The structures of **1**−**4** were determined by single-crystal X-ray diffraction analyses (Table 1). The crystal structures of the coordination polymers **1**−**4** comprise a 2D honeycomb-type framework, as shown in Figure 1. Compounds Ln−Mn (**1** and **2**) and Ln−Zn (**3** and **4**) crystallized in the rhombohedral crystal system, space group $R\bar{3}$. The 2D coordination network of **1** is shown in Figure 2. The Ho^{3+} ion is coordinated by three tridentate (ONO) HCAM anions to form a tricapped trigonal prism, and the average bond lengths of Ho−O and Ho−N are 2.402 and 2.471 Å, respectively. The coordination geometry around the Mn^{2+} center is a slightly distorted octahedron. Four water molecules construct the equatorial plane of the Mn^{2+} center with an average Mn−O bond length of 2.195 Å, and two carboxylic O atoms occupy the remaining apical coordinate sites with a Mn−O distance of 2.141 Å. Each HCAM molecule chelates to one Ho^{3+} ion and links to one Mn^{2+} ion. Therefore, each Ho center has three Mn^{2+} ions as the nearest metal centers, while the Mn center has two Ho^{3+} ions in its vicinity, as is consistent with the Mn/Ho molar ratio (3:2). As a result, the formation of a metallocycle with a diameter of about 1.4 nm (defined as the distance between two opposite Mn^{2+} ions) shows a 48MR comprising six Ln, six Mn, 12 C, and 24 O atoms, of which, the Ln and Mn atoms are arrayed alternatively and connected by O−C−O bridges (Figure 1). These 48MRs as building blocks, linked via carboxyl bridges, construct a 2D honeycomb coordination layer. These 2D honeycomb layers are packed in the ABCABC sequence along the c direction, and there are no open channels in **1**−**4**. Coordination polymers exhibiting 2D honeycomb-shaped or hexagonal networks, structural analogues of graphite, normally containing transition metal ions

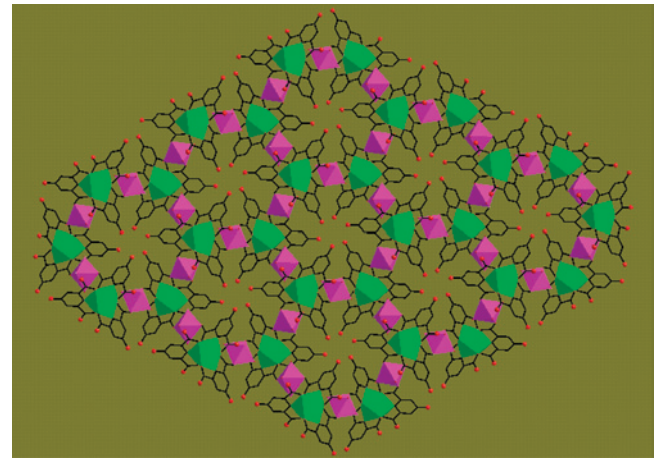

Figure 1. Diamond view of 2D honeycomb layers along the c axis in **1**−**4**. Red, O; green, Er or Ho; purple, Mn or Zn; blue, N; black, C. H atoms are omitted for clarity.

(10) (a) Sheldrick, G. M. *SHELXL-97*; University of Göttingen: Göttingen, Germany, 1997. (b) Sheldrick, G. M. *SHELXL-97*; University of Göttingen: Göttingen, Germany, 1997.
(11) Ramón, J.; Mascarós, G.; Dunbar, K. R. *Angew. Chem., Int. Ed.* **2003**, *42*, 2289.
(12) Liu, C. W.; Liaw, B. J.; Liou, L. S.; Wang, J. C. *Chem. Commun.* **2005**, 1983.
(13) Kepert, C. J.; Prior, T. J.; Rosseinsky, M. J. *J. Solid State Chem.* **2000**, *152*, 261.

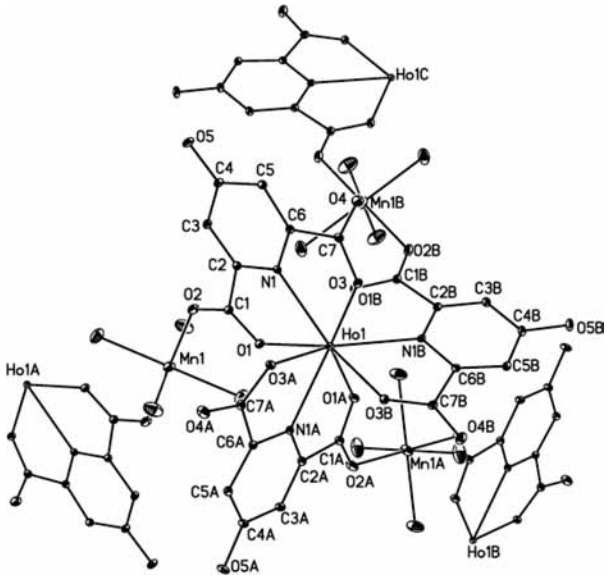

Figure 2. Diagram showing the building units with atom labels in **1**. H atoms are omitted for clarity. Symmetry operations: (A) $-x + y + 1, -x + 1, z$. (B) $-y + 1, x - y, z$. (C) $-x + 2, -y + 1, -z$.

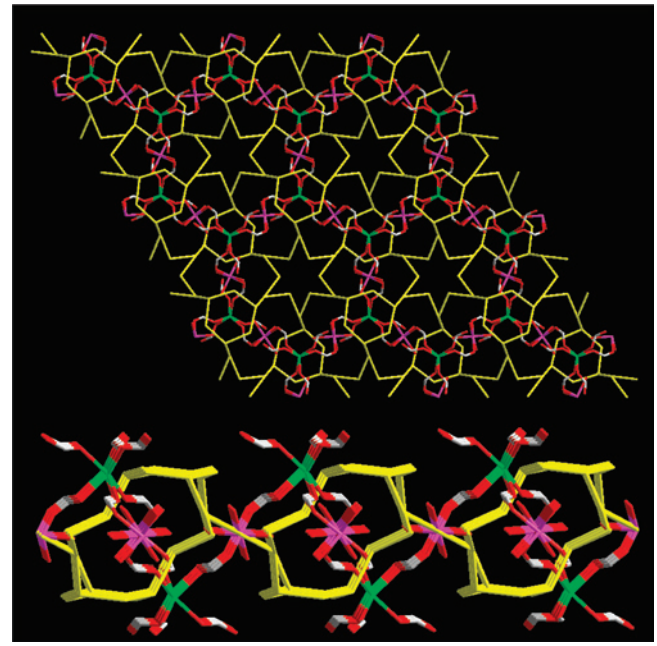

Figure 3. Perspective view showing the interpenetration of the 2D water sheet and 2D coordination layer in **3** and **4**. Red, O; green, Er or Ho; purple, Mn or Zn; white, C; yellow layer, water sheet. The C atoms of the pyridine rings and the H atoms and O atoms of phenol are omitted for clarity.

(such as Co,[11] Ag[12] or Ni[13]) and lanthanide ions[14] with various MRs or organic molecules[15] are well documented; however, to the best of our knowledge, 3d−4f 48MRs in honeycomb-shaped networks have not been previously observed.

Another interesting point of the structures is the cocrystallized water molecules. The 2D coordination layers contain the coordination water molecules, the −OH groups of HCAM ligands, and the O atoms of carboxyl groups as hydrogen-bonding donors or acceptors, which act as host templates with the hope of encapsulating water clusters within their crystal lattices. Compounds **3** and **4** contain an ordered 2D hydrogen-bonded icelike sheet (Figure 3). Hydrogen-bonding association generates six-membered and 12-membered water rings, which are further assembled to a 2D supramolecular icelike morphology with a corrugated sheet. The O···O distances in the hydrogen bonds found in this supramolecular structure of water range from 2.754 to 2.877 Å (**3**) and from 2.766 to 2.883 Å (**4**), with average values of 2.808 and 2.798 Å, respectively. For comparison, the O···O separations in ice I_h[16] and liquid water are 2.75 and 2.85 Å,[17] respectively. The $(H_2O)_6$ rings exist up and down the 2D coordination layer. This is the first 2D water found to exist in 3d−4f compounds. Due to higher synthesis temperature in **1** and **2**, less water molecules cocrystallize with the coordination frameworks, and these water molecules form small water clusters rather than a polymeric structure. Recently, 2D water/ice sheets containing six-,[18] 12-[19] or 18-membered[20] water rings have been observed in solid states; to our knowledge, the 2D water sheet constructed via mixed six- and 12-membered water rings have never been observed in water chemistry.

Thermal Gravimetric Analyses (TGA). The results from the thermogravemetric analysis of **2** and **4** performed under conditions between 25 and 600 °C are very similar (Supporting Information). However, the release of uncoordinated water molecules is easier in **2** than for **4**. The first step of weight loss on **4** between room temperature and 250 °C corresponds to nine lattice water molecules. The uncoordination water molecules are not released completely until 400 °C is reached. These data reveal that the 2D ice sheets in **4** are partly destroyed until 250 °C is reached, and the host coordination networks hold some water molecules of these 2D ice sheets more strongly than others. The further weight loss until 600 °C indicates the decomposition of **4**.

Magnetic Properties. The magnetic susceptibility measurements of **1**−**4** have been performed on a Quantum Design MPMS-5S SQUID magnetometer at 1000 Oe in the 2−300 K temperature range. The diamagnetic correction was evaluated by using Pascal's constants. In order to investigate the magnetic interaction between Ln and Mn ions, the method of diamagnetic ions substitution was applied on the basis of the following considerations:[7,8] (1) In this work, the ligand fields of Ln in the Ln−Mn and the Ln−Zn species may be considered approximately identical due to the same valence state and analogous ion radius of Mn^{2+} and Zn^{2+}. (2) The magnetic coupling between adjacent Mn^{2+} may be ignored because of the long distance between them of 7.226 Å. As a result, the comparison between isomorphous Ln−Mn

(14) Zaworotko, M. J. *Chem. Commun.* **2001**, 1.
(15) Batten, S. R.; Robson, R. *Angew. Chem., Int. Ed.* **1998**, *37*, 1460.
(16) The value is taken from the data at 200 K: Eisenbery, D.; Kauzmann, W. *The Structure and Properties of Water*; Oxford University Press: Oxford, U.K., 1969.
(17) Narten, A. H.; Thiessen, W. E.; Blum, L. *Science* **1982**, *217*, 1033.
(18) Cuamatzi, P. R.; Vargas-Diaz, G.; Höpfl, H. *Angew. Chem., Int. Ed.* **2004**, *43*, 3041.
(19) Janiak, C.; Scharman, T. G. *J. Am. Chem. Soc.* **2002**, *124*, 14010.
(20) Raghuraman, K.; Katti, K. K.; Barbour, L. J.; Pillarsetty, N.; Barnes, C. L.; Katti, K. V. *J. Am. Chem. Soc.* **2003**, *125*, 6955.

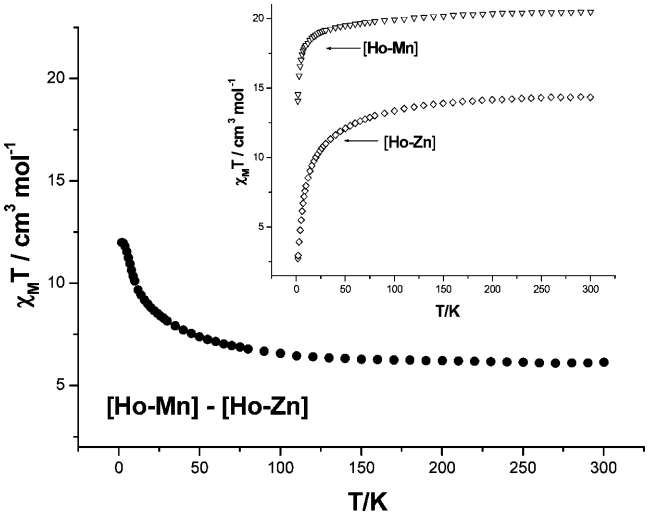

Figure 4. Result of the subtraction of the Ho^{3+} paramagnetic contribution of **1**. Inset is $\chi_M T$ versus T plot for compounds **1** and **3** under 1000 Oe.

and Ln−Zn complexes, which is defined as a function $\Delta(\chi_M T) = (\chi_M T)_{Ln-Mn} - (\chi_M T)_{Ln-Zn}$, may eliminate the crystal field contribution of Ln ions. Thus, according to the change trend of $\Delta(\chi_M T)$ in the 2−300 K temperature range, the ferromagnetic or antiferromagnetic coupling between adjacent Ln^{3+} and Mn^{2+} would be clearly concluded.

As shown in Figure 4, the observed $\chi_M T$ values for **1** and **3** at 300 K are 20.48 and 14.34 $cm^3\ mol^{-1}$ K, respectively, slightly smaller than the calculated values of 20.63 and 14.53 $cm^3\ mol^{-1}$ K for the uncorrelated magnetic moments of one Ho^{3+} and one and half Mn^{2+} ions, respectively. As the temperature was lowered, $\chi_M T$ values decreased more and more rapidly to reach 14.04 and 2.73 $cm^3\ mol^{-1}$ K for **1** and **3**, respcetively. Interestingly, the curves of $(\chi_M T)_{Ho-Mn}$ and $(\chi_M T)_{Ho-Zn}$ versus T are roughly parallel from 300 to 125 K, and in the temperature range used, the difference $\Delta(\chi_M T)$ almost stays constant. These observations indicate that the decreases of $(\chi_M T)_{Ho-Mn}$ and $(\chi_M T)_{Ho-Zn}$ must be considered as intrinsic characteristics of the Ho^{3+} ions and must be essentially attributed to the depopulation of the Stark levels. The isomorphism between **1** and **3** supports the view that, for a given rare earth ion, the same crystal field is operative in both complexes, which gives rise to the same distribution of Stark levels. Below 125 K, $\Delta(\chi_M T)$ increases steadily to reach a maximum of 11.99 $cm^3\ mol^{-1}$ K at 2 K. The profile of the curve clearly shows that ferromagnetic interaction takes place between the Ho^{3+} and Mn^{2+} ions within **1**.

The observed $\chi_M T$ values for **2** and **4** at 300 K are 18.22 and 11.81 $cm^3\ mol^{-1}$ K, respectively, slightly higher than the calculated values of 17.58 and 11.48 $cm^3\ mol^{-1}$ K for noninteracting free ions per $ErMn_{1.5}$ and $ErZn_{1.5}$ unit, respectively (Figure 5). Upon cooling, the $\chi_M T$ of **2** increases more and more rapidly from 300 to 19 K to reach a maximum of 19.71 $cm^3\ mol^{-1}$ K and then decreases rapidly to reach 16.09 $cm^3\ mol^{-1}$ K at 2 K. The increase of $\chi_M T$ with cooling is characteristic of an enlargement of the total magnetic moment of the molecules, as a result of ferromagnetic interaction between the spin carriers. At 300 K, $\Delta(\chi_M T)$ is equal to 6.41 $cm^3\ mol^{-1}$ K, the expected value for one and a half noncorrelated $S_{Mn} = 5/2$ spins, and increases constantly as T is lowered to reach a maximum of 7.97 $cm^3\ mol^{-1}$ K at 19 K. Below this temperature, $\Delta(\chi_M T)$ decreases rapidly to about 5.02 $cm^3\ mol^{-1}$ K at 2 K. From 300 to 19 K, the increase of $\Delta(\chi_M T)$ indicates ferromagnetic interactions between Er^{3+} and Mn^{2+} ions within **2**. The decrease of $\Delta(\chi_M T)$ from 19 to 2 K might be due to intermolecular antiferromagnetic interactions, or zero-field splitting of Mn^{2+} ions.

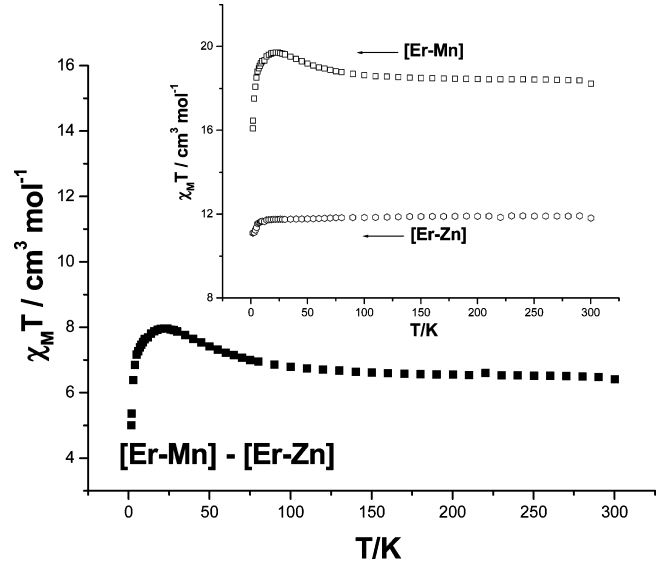

Figure 5. Result of the subtraction of the Er^{3+} paramagnetic contribution of **2**. Inset is $\chi_M T$ versus T plot for compounds **2** and **4** under 1000 Oe.

Conclusions

In summary, four 3d−4f heterometallic coordination polymers are successfully synthesized under hydrothermal conditions. Structural analyses reveal that **1**−**4** comprise a 2D honeycomb-type framework. A 2D water sheet is first found in **3** and **4**, which exhibits a novel topological motif in water chemistry. Interestingly, the ferromagnetic interaction between Mn^{2+} and Ho^{3+} (or Er^{3+}) has been demonstrated. The extension of this study to the other paramagnetic Ln^{3+} ions and the second spin carrier will allow us to gain some insight into the basic information about magnetic interactions involving rare earth metals and, consequently, to improve their use in the molecular approach to magnetic materials.

Acknowledgment. This work was supported by the National Natural Science Foundation of China (Nos. 20425103, 20501012 and 20631030), FANEDD (200732), NCET (07-0463), and 973 Program 2007CB815305.

Supporting Information Available: X-ray crystallographic files (CIF) for **1**−**4**. This material is available free of charge via the Internet at http//pubs.acs.org.

IC801332A